**Reprint**

J.M. Costa, A.N. Venetsanopoulos and M. Trefler, "Digital tomographic filtering of radiographs", *IEEE Transactions on Medical Imaging*, Vol. MI-2, No. 2, pp. 76-88, June 1983.

# Digital Tomographic Filtering of Radiographs

JOSÉ M. COSTA, ANASTASIOS N. VENETSANOPOULOS, AND MARTIN TREFLER

*Abstract*—**Conventional radiographs do not provide information about the depths of details and structures because they are two-dimensional projections of three-dimensional bodies. Taking advantage of the finite size of the X-ray source and the divergent nature of the X-ray beam, a radiograph can be processed by two-dimensional digital filtering techniques, so that the image of a particular layer is improved, while the others are degraded. This technique is referred to as a tomographic filtration process (TFP). This paper develops the mathematical and physical foundations of the method. Based on a model of the radiologic process, which is described in the paper, the equations of image formation in standard tomography, conventional radiography, and tomographic filtering are derived and compared.**

## I. Introduction

THE problem of imaging three-dimensional bodies and obtaining information about the depth of details and structures has been recognized for a long time. As early as 1916 special radiographic procedures were invented to obtain clear images of certain parts of an object by blurring images from other parts [1]. These procedures will be referred to throughout this paper as *standard tomography*. More recently, significant advancements have been made in computer-assisted tomography (CAT) and coded aperture imaging [2]. One of the remaining challenges is to improve the diagnostic value of the billions of radiographs being produced in hospitals every year using conventional radiography equipment. *Conventional radiography* does not include special techniques that will highlight single layers in the body being imaged. Enhancement and restoration techniques have had limited practical application to the processing of radiographs [2]. With digital radiography, techniques that had only been used in lab experiments could now be applied much more readily. However, little work has been published on the problem of recovering three-dimensional information from a single radiograph (cf. [3]).

The purpose of this paper is to present a procedure for improving three-dimensional information in a radiograph using digital techniques. This method has been referred to as *tomographic filtering* or a *tomographic filtration process* (TFP) [4]-[6].

An analysis of the radiologic process has shown that two factors that could be useful for obtaining three-dimensional information are due to the finite size of the focal spot and the diverging nature of the X-ray beam [6]. Indeed, due to the finite size of the focal spot, there is a blur associated with the image of each layer, which is depth-dependent. This suggests that there could be some kind of selective restoration of each layer's image (tomographic restoration). Also, the diverging nature of the X-ray beam has the effect of magnifying each layer in the film so that the spectra of the layers are scaled differently. This suggests that selective enhancement of the layers could be realized by means of spectral shaping filters (tomographic enhancement).

This approach to tomographic restoration of radiographs uses the depth-dependent focal spot blur. Section II describes the model of the radiologic process, on which the development of a TFP is based. The TFP itself is developed in Section III, where the mathematics of standard tomography, conventional radiology and TFP are derived and compared. Sections IV to VI contain further analyses of TFP, in Section IV the transfer function of a TFP is compared with that of standard tomography and conventional radiology, in Section V evaluations in terms of quantitative performance parameters are summarized, and in Section VI the effect of a TFP at various depths is analyzed.

## II. Model of the Radiologic Process

Before any improvement of radiographs can be attempted, it is necessary to study the characteristics of the image formation process to find out what the depth-dependent features are. To date, almost all theory of conventional radiography has dealt with two-dimensional objects (cf. [7]). The very nature of the radiologic process, however, forces one to consider three-dimensional objects in all imaging problems. The radiographic process consists of a sequence of transformations intimately related in that the result of one forms the input to the next [8]. The degradations introduced at each stage of the radiologic process has been studied in great detail from the viewpoint of image quality (e.g., [8]-[12]).

Fig. 1 shows a block diagram model of the radiologic process. In general, block inputs and outputs are two-dimensional functions representing distributions of intensities. Unless otherwise specified, we will deal with intensity images rather than density images[1]. The operation in each block can be represented by mathematical equations relating the output to the input. There are many factors, especially those which are random in nature, not taken into account in the block diagram of Fig. 1(a). These factors are considered to be noise and they are modeled by a

Manuscript received March 16, 1983; revised July 28, 1983.

J. M. Costa is with Bell-Northern Research, Ottawa, Ont., Canada K1Y 4H7.

A. N. Venetsanopoulos is with the Department of Electrical Engineering, University of Toronto, Toronto, Ont., Canada M5S 1A4.

M. Trefler is with the Department of Radiology, Division of Radiological Sciences, School of Medicine, University of Miami, Miami, FL 33101.

[1] An intensity image is defined to be an image represented by values which are linearly proportional to the intensity of the original radiant energy component involved in the image formation. A density image is defined as an image in which the values are proportional to the logarithm of the intensity of the original radiant energy component involved in the image formation [13].

0278-0062/83/0600-0076$01.00 

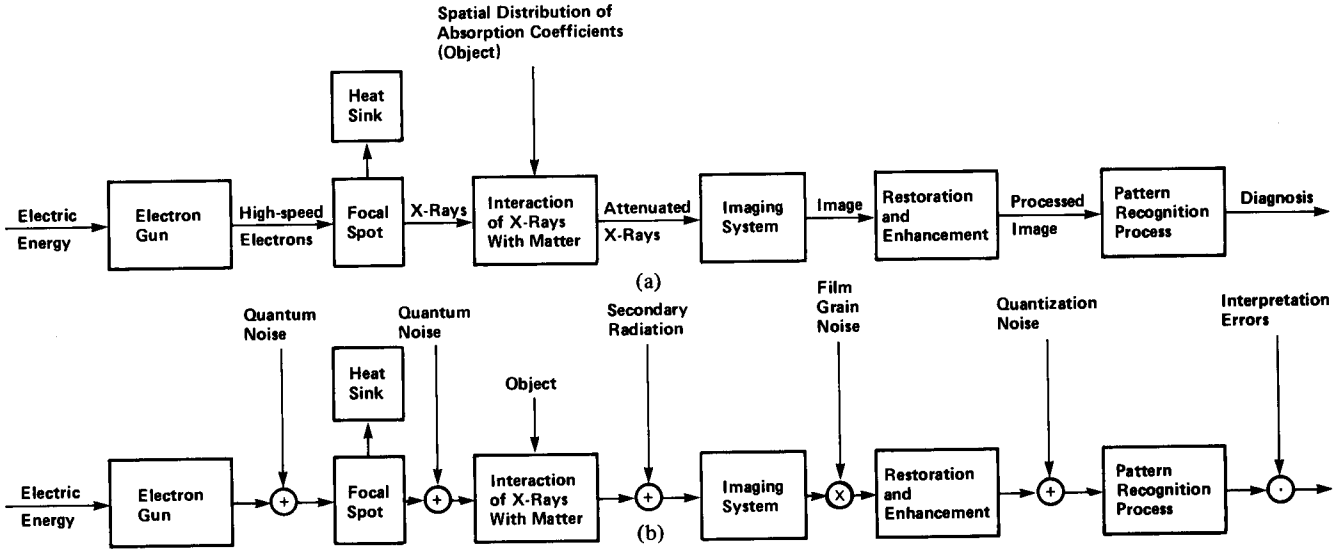


Fig. 1. Block diagram model of the radiologic process. (a) Noiseless. (b) With noise.

perturbing noise source at the output of each block in Fig. 1(b). The manner in which the noise is combined with the image depends on how the image has been formed and the nature of the noise process. Usually, additive or multiplicative noise is assumed.

The *electron gun* consists of a cathode emitting electrons, which are focused and accelerated at high speed towards the anode. The input to this block is electric energy and the output is the spatial distribution of the current of high-speed electrons. The region in the target where the X-rays and heat are produced is called the *focal spot*. The angle formed by the target surface and the direction of the center X-ray is referred to as the target angle. The intensity of the radiation tends to be greater in the direction of movement of the electrons; however, for applied voltages in the 50-150 kV range, used in diagnostic radiology, X-rays are emitted more or less uniformly in all directions.

Many studies have been published about the characteristics of focal spots in X-ray tubes (e.g., [14]-[19]). The shape and size of focal spots have been determined as well as their modulation transfer functions (MTF's) and point-spread functions (PTF's), both theoretically and experimentally. Nevertheless, for mathematical simplicity, many researchers assume that the focal spot can be represented by a geometrical shape (e.g., a square or a circle) with definite edges. In this case the MTF of a focal spot is some form of a two-dimensional sampling function. Real focal spots do not have sharp edges, rather there is an edge gradient shaped like a Gaussian function. Indeed, it has been stated in the literature [14], [17], [20] that the MTF of a focal spot resembles more a Gaussian function rather than a sampling function and that this approximation is better in certain directions than others. A spatial Gaussian function seems a good approximation to the spatial distribution of X-rays. When the source of electrons is of finite size, the resulting distribution of X-rays is an image of the filament with the edges approximated by Gaussian functions. Since our purpose is not the design of radiologic systems but the design of filters that will compensate for the degradations in existing systems, we will assume that the output of the focal spot block, that is, the distribution of X-rays emitted by the focal spot, can be measured. Therefore, we will not consider any further the characteristics of the first two blocks.

The *interaction of X-rays with matter* (attenuation) may be modeled by the differential equation in (1), where $I(x)$ is the intensity of a narrow X-ray beam as a function of the distance $x$ in the direction of propagation and $\mu(x)$ is a total linear attenuation coefficient

$$\frac{dI(x)}{dx} + \mu(x)\, I(x) = 0. \tag{1}$$

The solution of (1) is given in (2):

$$I(x) = I(0) \exp\left(-\int_o^x \mu(\sigma)\, d\sigma\right). \tag{2}$$

X-rays propagate in straight lines. This fact controls the size, shape, and position on the radiographic film of the shadow or image of the various structures of the object being exposed. The ratio of the size of the image to that of the object is called the magnification. For a three-dimensional object, the magnification is a constant in a layer parallel to the film plane. If we denote by $d_1$, the distance from the focal spot to the $i$th layer, and by $d_2$, the distance from that layer to the film plane, the magnification for that layer is given by

$$m_i = \frac{d_1 + d_2}{d_1}. \tag{3}$$

The X-ray intensity distribution that reaches the imaging system is a function of both the object and the X-ray intensity distribution in the focal spot. To maintain generality in our block diagram, we model the interaction of X-rays with matter as a system with two inputs.

We denote by $I_o(x_o, y_o; x, y)$ the X-ray intensity emitted from the point $(x_o, y_o)$ in the focal spot toward the point $(x,y)$ in the film plane. The other input is denoted by $\mu_L(l)$ and corresponds to the spatial distribution of absorption coefficients in the object. $\mu_L(l)$ is defined along a line $L$ from $(x_o, y_o)$ to $(x, y)$.

The interaction between these two inputs can then be modeled by the following integral equation:

$$I(x,y) = \iint_{FS} I_o(x_o, y_o; x, y) \cdot \exp\left(-\int_L \mu_L(l)\, dl\right) dx_o\, dy_o \quad (4)$$

which is a generalization of (2) and is obtained by integrating over the region of existence of the focal spot (denoted here by FS). The integral in the exponential is along a line $L$ defined by the point $(x_o, y_o)$ in the focal spot and the point $(x, y)$ in the film plane.

A pragmatic approach to conventional radiographic image formation systems has been dominant in past efforts in this field [13]; namely, a linear space-invariant model is assumed. The thickness of the object is neglected and the point-spread function is estimated by approximations. The space-variant model is considered in the Appendix, where a solution is proposed to convert the space-variant model into a space-invariant one. The salient feature of (4), as well as of subsequent equations which will be derived from (4), is that it shows what happens when X-rays are attenuated by three-dimensional objects, thus setting the basis for the recovery and separation of the information which is projected on the film. Other effects such as the inverse square law and scattered radiation are not relevant here because they do not contribute to differentiate among layers. The integrals in (4) can be approximated by summations. This discretization is suitable for implementation in a digital computer and is useful in performing simulations. For this purpose we coded the routine XRAY in Fortran IV. The details are given in [6].

Due to the finite size of the focal spot, the shadow image of a point or edge in the object extends over a finite region on the film plane. Each edge or shadow is composed of two parts, the umbra and the penumbra or edge gradient[2]. These effects will be discussed further and exploited to derive the basis of tomographic filtering.

Several researchers have investigated the removal of penumbras in radiographs using optical signal processing techniques (Minkoff [22], Krusos [23], and Trefler [24]).

When X-rays interact with matter, they are not only attenuated in intensity, but also they are scattered through a finite solid angle tending to produce a hazy background in the image only indirectly related to absorption coefficients in the object [25]. Therefore, we model this secondary radiation as additive noise. The problem of estimating the PSF due to radiation scattering and the realization of a compensating filter using digital techniques has been studied by Hunt [26], [27].

The *imaging system* is the conversion process of an X-ray image to a light image. Image intensifiers or screens are used for that purpose. These imaging devices introduce degradations which can be characterized by their PSF's on their frequency responses. The input to the imaging system is the X-ray intensity distribution just before it enters a screen-film combination or an image intensifier and the output is a film image or a television image, respectively.

In addition to the low-pass characteristics of the frequency response of the imaging device, the main distortions in the recording and display of images are due to random noise and nonlinearities. The main characteristic of this kind of noise is that it appears to be multiplicative rather that additive [28] [13]. If the images are sampled somewhere in the process, nonlinearities can be compensated for in a digital computer [13]. All these effects have been studied in detail by several authors [13], [28]-[31].

*Restoration and enhancement*, which are not normally present in conventional radiologic systems, are the principal objectives of this research. Given the characteristics of all other blocks, we have to design the restoration and enhancement methods that will improve the final output of the whole system, i.e., the diagnosis.

Restoration refers to that part of the system that corrects for degradations in other parts of the process. The design of the restoration filter requires knowledge of the degradations in the system, that is the transfer functions of the previous blocks. The way this knowledge is acquired may be represented in the block diagram by a feedforward path.

By enhancement we refer to the processing of images in general, to present to the viewer (or subsequent machine) additional information or insight into some factor concerning the preenhanced image. A comprehensive survey of image enhancement techniques has been published by Andrews [32]. It must be emphasized that the fidelity criterion of enhancement is not attempting better object representation; it will depend strongly on the type of pattern recognition process (PRP) used and on the relevant features in the image. If the PRP is automated, a mathematical criterion like the mean-square error will be in order; but if the image is to be viewed by a human viewer, such as the radiologist, then the psychophysics of vision and other human factors must be taken into account [30], [33]. Therefore, the design of an enhancement filter needs a feedback of the characteristics of the PRP following it.

The *Pattern Recognition Process (PRP)* is the ultimate and most intelligent system block in the whole process which results in the diagnosis. The pattern recognition may be performed by an automated process, a radiologist, or both in combination. For a survey of automated PRP techniques for radiographs see, for example, Hall [34].

## III. A Tomographic Filtration Process

### A. Analogy with Standard Tomography

Standard tomographic techniques produce a tomogram by moving a point-like X-ray source and the recording film in a coupled manner, so that during the exposure the parts of the object lying in one specific plane parallel to the film plane are always projected on the same place on the film [1]. The X-ray shadows of the other parts of the object will move in relation

[2] Umbra is defined as the zone of lucence formed on a film when a radiopaque object intervenes between the film and a source emitting X-rays. Penumbra, or more accurately edge gradient, is defined as the gradation in density which occurs at the margin of any given radiological image, delineated medially by the point of maximum image lucence and laterally by the point of minimum image lucence [21].

to the film. Thus a layer of finite thickness at a predefined depth of the body is imaged sharply, whereas structures on both sides of this layer are blurred. The layer whose image is in focus is referred to as the plane of cut or tomographic layer.

A tomographic filtration process (TFP) must produce a focussing effect similar to that of standard tomography, but with no moving parts. In a TFP, instead of moving the X-ray tube, the finite size of the focal spot is used to advantage, and instead of moving the film, a filter is used to process a conventional radiograph. To see that a TFP is indeed analogous to a standard tomographic system in miniature, as far as the tomographic layer is concerned, consider the following model.

A focal spot is composed of a finite ordering of point sources. Each emitting source produces its own image at a slightly different point in the image plane. The shadow from all these point sources add up to form the observed image; overlapping occurs throughout the entire image, but will only be discernible at the edges where an intensity gradient is formed.

Since this system is linear we can apply superposition and make an equivalent focal spot by moving a true point source of X-rays over a region which includes the real focal spot. With this model, (4) is still valid.

The movement of this point source is analogous to the movement of an X-ray tube in standard tomography. Since in conventional radiology the film does not move, the images of all the layers are blurred. Therefore, in order to convert a radiograph into a tomogram we will pass the radiographic image through a filter. Filters that produce a selective deblurring on a conventional radiograph will be referred to as tomographic filters.

Since a typical size for the focal spot is of the order of 2 mm, while the movement of an X-ray source in standard tomography is of the order of 500 mm, we infer that a TFP would be more comparable to zonography. Zonography is essentially standard tomography using small displacements of the X-ray source, of the order of a few mm [35, p. 360], [36, ch. 14], [37], [38]. Other comparable narrow-angle tomographic techniques are stereo zonography, narrow angle stratigraphy, and orthotomography [36, pp. 7-8, 300-311].

### *B. The Mathematics of Tomographic Filtering*

In order to derive the characteristics of a tomographic filtration process, the mathematics of standard tomography, conventional radiology, and tomographic filtering are studied in depth and compared.

*A Mathematical Model of Standard Tomography:* The derivation first of an equation describing the image formation process in standard tomography will serve to derive the equation of image formation in conventional radiology and to compare tomographic filtering with standard tomography.

This derivation was motivated by that in [39]. We have removed some of the constraints in [39] (namely, the linear movement of a constant intensity X-ray source), while we have added others relevant to this application (namely, small displacements of the X-ray source). Nevertheless, none of these constraints imply a lack of generality in the derivation.

Consider the diagram of standard tomography in Fig. 2. In our model, the punctual X-ray source can move anywhere in a plane parallel to the film. This movement can be linear, circular, spiral, etc., even the scanning of an area may be considered. Generally, the intensity $I_o$ of the X-ray source may change with its location. In standard tomography the film also moves in synchronism with the X-ray source to keep the desired plane of cut in focus.

Suppose a reference coordinate system $x, y, z$ with origin at $O$. The coordinates of a point in a plane at a depth $z_i$ are denoted by $(x_i, y_i)$. Let $\Delta_1$ and $d$ be the distance from the X-ray source to the plane of cut and to the film, respectively. Thus, $\Delta_2 \triangleq d - \Delta_1$ is the distance from the plane of cut to the film.

When the source of X-rays is at $(x_o, y_o)$, the coordinates of the center of the film $(x_c, y_c)$ are given in (5):

$$x_c = K x_o \tag{5a}$$

$$y_c = K y_o \tag{5b}$$

where

$$K = -\Delta_2/\Delta_1. \tag{6}$$

Thus, the relationship between the absolute coordinates $(x, y)$ on the film plane and the coordinates $(x_f, y_f)$ of a point in the film with respect to the center of the film is given by

$$x = x_c + x_f = K x_o + x_f \tag{7a}$$

$$y = y_c + y_f = K y_o + y_f. \tag{7b}$$

The coordinates $(x_i, y_i, z_i)$ of any point in the space between the film and the focal spot can be expressed as a function of $(x_o, y_o)$–the point of origin of the X-ray passing through $(x_i, y_i, z_i)$, and $(x_f, y_f)$–the point of impact of the X-ray on the film:

$$x_i = \frac{(z_i - \Delta_2)x_o}{\Delta_1} + \frac{d - z_i}{d} x_f \tag{8a}$$

$$y_i = \frac{(z_i - \Delta_2)y_o}{\Delta_1} + \frac{d - z_i}{d} y_f. \tag{8b}$$

For a punctual source of X-rays at $(x_o, y_o)$ emitting an intensity $I_o(x_o, y_o; x_f, y_f)$ towards the point $(x_f, y_f)$ on the film, the intensity $I(x_f, y_f; x_o, y_o)$ reaching that point is [cf. (2)]

$$I(x_f, y_f; x_o, y_o) = I_o(x_o, y_o; x_f, y_f) \cdot \exp\left\{-\int_s \mu(x_i, y_i, z_i)\, ds\right\} \tag{9}$$

where $\mu(x_i, y_i, z_i)$ is the function representing the distribution of linear attenuation coefficients and $s$ denotes the path between $(x_o, y_o)$ and $(x_f, y_f)$.

*Approximations:*

1) $I_o(x_o, y_o; x_f, y_f)$ can be assumed with good approximation independent of $(x_f, y_f)$ [39]. Thus, $I_o(x_o, y_o; x_f, y_f) \simeq I_o(x_o, y_o)$.

2) $ds$ is replaced by $dz_i$:

$$ds = \frac{dz_i}{\cos\theta'} \simeq \frac{dz_i}{\cos\theta} = \sqrt{1 + \tan^2\theta}\, dz_i = \sqrt{1 + \frac{x_o^2 + y_o^2}{\Delta_1^2}}\, dz_i.$$

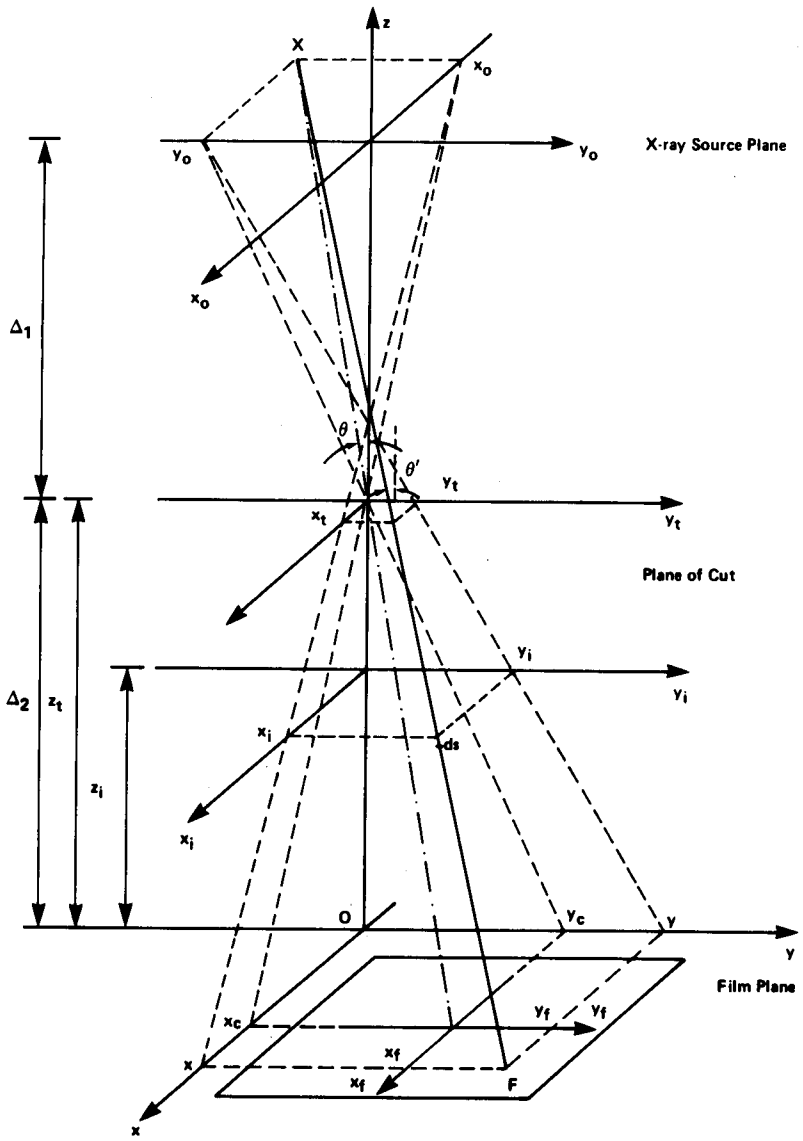


Fig. 2. Diagram of standard tomography.

If the displacements of the X-ray source are small compared to the distance from the X-ray source to the plane of cut, then $x_o, y_o \ll \Delta_1$, in which case $ds \simeq dz_i$.

3) Since the values of the linear attenuation coefficients, or at least their variations from point to point, are small, the exponential in (9) can be approximated by the linear terms of its Taylor series expansion[3] [39].

Therefore, taking into account all these approximations, (9) becomes

$$I(x_f, y_f; x_o, y_o) = I_o(x_o, y_o) \left[1 - \int_0^d \mu(x_i, y_i, z_i)\, dz_i\right]. \tag{10}$$

When the source of X-rays moves and its intensity is given by $I_o(x_o, y_o)$ while the film also moves simultaneously as defined in (7), the total intensity after the exposure at any point $(x_f, y_f)$ on the film is

$$\begin{aligned} I(x_f, y_f) &= \iint I(x_f, y_f; x_o, y_o)\, dx_o\, dy_o \\ &= \iint I_o(x_o, y_o) \left[1 - \int_0^d \mu(x_i, y_i, z_i)\, dz_i\right] \\ &\quad \cdot dx_o\, dy_o \\ &= I_B - \int_0^d I_i(x_f, y_f, z_i)\, dz_i \end{aligned} \tag{11}$$

where

$$I_B = \iint I_o(x_o, y_o)\, dx_o\, dy_o \tag{12a}$$

$$I_i(x_f, y_f, z_i) = \iint I_o(x_o, y_o)\, \mu(x_i, y_i, z_i)\, dx_o\, dy_o \tag{12b}$$

and the values of $x_i$ and $y_i$ are given in (8) as a function of $x_o$, $y_o$, $x_f$, $y_f$, and $z_i$.

[3]The validity of this assumption has been investigated by Orphanoudakis *et al.*, who concluded that, to describe linear tomography, a Fourier decomposition approach leading to an MTF is reasonable, though there are a few situations where a nonlinear analysis might be significantly more accurate [41].

Replacing (8) into (12b) and making a change of variables[4], we obtain

$$I_i(x_f, y_f, z_i) = K_i^2 \iint I_o(K_i\xi, K_i\eta) \cdot \mu\left(\frac{d - z_i}{d}(x_f - \xi), \frac{d - z_i}{d}(y_f - \eta), z_i\right) d\xi\, d\eta \qquad (13)$$

where

$$K_i = \frac{z_i - d}{z_i - \Delta_2}\,\frac{\Delta_1}{d}. \qquad (14)$$

Since (13) is a convolution, in the frequency domain it becomes a product:

$$G_i(f_x, f_y, z_i) = H_i(f_x, f_y, z_i)\, F_\mu(f_x, f_y, z_i) \qquad (15)$$

where

$$G_i(f_x, f_y, z_i) = \iint I_i(x, y, z_i)\, e^{-j2\pi(f_x x + f_y y)}\, dx\, dy \qquad (16)$$

$$H_i(f_x, f_y, z_i) = K_i^2 \iint I_o\left(\frac{z_i - d}{z_i - \Delta_2}\,\frac{\Delta_1}{d}\,x, \frac{z_i - d}{z_i - \Delta_2}\,\frac{\Delta_1}{d}\,y\right) \cdot e^{-j2\pi(f_x x + f_y y)}\, dx\, dy \qquad (17)$$

$$F_\mu(f_x, f_y, z_i) = \iint \mu\left(\frac{d - z_i}{d}\,x, \frac{d - z_i}{d}\,y, z_i\right) \cdot e^{-j2\pi(f_x x + f_y y)}\, dx\, dy. \qquad (18)$$

Replacing (15) into the Fourier transform of (11) we obtain (19):

$$G(f_x, f_y) = I_B\,\delta(f_x, f_y) - \int_0^d G_i(f_x, f_y, z_i)\, dz_i = I_B\,\delta(f_x, f_y) - \int_0^d H_i(f_x, f_y, z_i) \cdot F_\mu(f_x, f_y, z_i)\, dz_i \qquad (19)$$

where $G(f_x, f_y)$ is the Fourier transform of the tomogram $I(x_f, y_f)$ [cf. (11)] and $H_i(f_x, f_y, z_i)$ is the transfer function of the $i$th layer, at a distance $z_i$ from the film, as given in (17).

Equation (19) is the equation of standard tomography in the frequency domain. This result agrees with that in [39], with the appropriate changes of notation and assumptions.

*Change of the Plane of Cut by Filtering the Tomogram:* In our model of standard tomography the depth of the plane of cut is $z_i = \Delta_2$ (cf. Fig. 2). As

$$z_i \to \Delta_2, \quad I_o\left(\frac{z_i - d}{z_i - \Delta_2}\,\frac{\Delta_1}{d}\,x, \frac{z_i - d}{z_i - \Delta_2}\,\frac{\Delta_1}{d}\,y\right)$$

in (17) approaches an impulse whose Fourier transform is a constant.

Thus, the transfer function of the plane of cut is a constant and its impulse response is an impulse, as expected by intuition (cf. Fig. 2).

Equation (19) suggests that we can change the plane of cut by filtering the tomogram. Indeed, suppose we are interested in the plane at a depth $z_i = z_t$. Dividing both sides of (19) by $H(f_x, f_y) \triangleq H_t(f_x, f_y, z_t)$, we obtain

$$\frac{G(f_x, f_y)}{H(f_x, f_y)} = I_B\,\frac{\delta(f_x, f_y)}{H(f_x, f_y)} - \int_0^d \frac{H_i(f_x, f_y, z_i)}{H(f_x, f_y)} \cdot F_\mu(f_x, f_y, z_i)\, dz_i. \qquad (20)$$

After filtering the tomogram with $H^{-1}(f_x, f_y)$, the overall transfer function for the layer at a depth $z_t$ is a constant, thus this layer has become the new plane of cut. The overall transfer function of the previous plane in focus ($z_i = \Delta_2$) is now $H^{-1}(f_x, f_y)$, namely, the filter transfer function. The overall transfer function for any other layer is

$$H_i(f_x, f_y, z_i) H^{-1}(f_x, f_y).$$

*A Mathematical Model of Conventional Radiology:* Consider a radiologic system with focal spot intensity distribution $I_o(x_o, y_o)$ and film to focal spot distance $d$. The diagram in Fig. 2 still applies if we let $\Delta_2 = 0$ and the movement of the punctual source of X-rays in standard tomography is replaced by the intensity distribution of the finite size focal spot. Under these conditions all the equations derived previously are still valid with $\Delta_2 = 0$.

The intensity on the film is given by (11), with $I_B$ as previously defined in (12a) and $I_i(x_f, y_f, z_f)$ as given in (21) [cf. (13)]:

$$I_i(x_f, y_f, z_i) = K_i^2 \iint I_o\left(\frac{z_i - d}{z_i}\,\xi, \frac{z_i - d}{z_i}\,\eta\right) \cdot \mu\left\{\frac{d - z_i}{d}(x_f - \xi), \frac{d - z_i}{d}(y_f - \eta), z_i\right\} d\xi\, d\eta. \qquad (21)$$

By letting $\mu(x, y) = \delta(x, y)$, an impulse, we obtain the impulse response of the $i$th layer.

In the frequency domain (15) and (19) are equally valid, but in conventional radiology the transfer function $H_i(f_x, f_y, z_i)$ of each layer is given by (22), [cf. (17) and let $\Delta_2 = 0$]:

$$H_i(f_x, f_y, z_i) = K_i^2 \iint I_o\left(\frac{z_i - d}{z_i}\,x, \frac{z_i - d}{z_i}\,y\right) \cdot e^{-j2\pi(f_x x + f_y y)}\, dx\, dy \qquad (22)$$

where

$$K_i = \frac{z_i - d}{z_i}.$$

Therefore, the mathematical models of standard tomography and conventional radiology are similar but with different transfer functions. In radiology none of the transfer functions is identically equal to a constant except in the limiting case that $z_i = 0$ (film plane).

*Tomographic Filtering of Radiographs:* As we did in (20) we can filter a radiograph so that the overall transfer function of one of the layers is equal to a constant, thus converting a radiograph into a tomogram. But now $H_i(f_x, f_y, z_i)$ is defined in (22) and

[4] $x_o = \frac{z_i - d}{z_i - \Delta_2}\,\frac{\Delta_1}{d}\,\xi$; and $y_o = \frac{z_i - d}{z_i - \Delta_2}\,\frac{\Delta_1}{d}\,\eta$.

$$H(f_x, f_y) = H_i(f_x, f_y, z_i)\big|_{i=t} = H_t(f_x, f_y, z_t)$$
$$= \left(\frac{z_t - d}{z_t}\right)^2 \iint I_o\left[\frac{z_t - d}{z_t}\, x, \frac{z_t - d}{z_t}\, y\right]$$
$$\cdot\, e^{-j2\pi(f_x x + f_y y)}\, dx\, dy. \tag{23}$$

Consequently, we have shown that by comparing the movement of a punctual X-ray source with a finite size focal spot and replacing the movement of the film in standard tomography by the filtration of a conventional radiograph, we can establish a conceptual analogy between standard tomography and tomographic filtering. In the following section this analogy is analyzed further.

## IV. Comparison of Transfer Functions

The frequency domain equation of image formation in radiology (24) was derived in the previous section [cf. (19)]:

$$G(f_x, f_y) = I_B\, \delta(f_x, f_y) - \int_0^d H_i(f_x, f_y, z_i)$$
$$\cdot\, F_\mu(f_x, f_y, z_i)\, dz_i \tag{24}$$

where $G(f_x, f_y)$ is the Fourier transform of the resulting image, $I_B$ is a constant, $H_i(f_x, f_y, z_i)$ is the overall transfer function of the $i$th layer at a depth $z_i$, and $F_\mu(f_x, f_y, z_i)$ is the Fourier transform of the (scaled) distribution of linear absorption coefficients in the $i$th layer [cf. (18)].

Equation (24) applies to standard tomography, conventional radiology, or tomographic filtering by using the transfer function given in (25), (26), or (27), respectively [cf. (17), (20), (22), and (23)].

*Standard Tomography:*

$$H_i^{ST}(f_x, f_y, z_i) = \left[\frac{z_i - d}{z_i - \Delta_2}\, \frac{\Delta_1}{d}\right]^2$$
$$\cdot \iint I_o\left\{\frac{z_i - d}{z_i - \Delta_2}\, \frac{\Delta_1}{d}\, x, \frac{z_i - d}{z_i - \Delta_2}\, \frac{\Delta_1}{d}\, y\right\}$$
$$\cdot\, e^{-j2\pi(f_x x + f_y y)}\, dx\, dy. \tag{25}$$

*Conventional Radiology:*

$$H_i^{CR}(f_x, f_y, z_i) = \left[\frac{z_i - d}{z_i}\right]^2 \iint I_o\left\{\frac{z_i - d}{z_i} x, \frac{z_i - d}{z_i} y\right\}$$
$$\cdot\, e^{-j2\pi(f_x x + f_y y)}\, dx\, dy. \tag{26}$$

*Tomographic Filtering:*

$$H_i^{TF}(f_x, f_y, z_i) = \frac{\left[\frac{z_i - d}{z_i}\right]^2 \iint I_o\left\{\frac{z_i - d}{z_i} x, \frac{z_i - d}{z_i} y\right\} e^{-j2\pi(f_x x + f_y y)}\, dx\, dy}{\left[\frac{z_t - d}{z_t}\right]^2 \iint I_o\left\{\frac{z_t - d}{z_t} x, \frac{z_t - d}{z_t} y\right\} e^{-j2\pi(f_x x + f_y y)}\, dx\, dy} \tag{27}$$

where the depth of the tomographic layer is $z_t = \Delta_2$, as usual.

In spite of the fact that the equations of image formation in standard tomography, conventional radiology, and tomographic filtering are similar, there are fundamental physical differences among these methods. A good objective indication of performance of a radiologic system is given by the overall transfer functions of the layers in the object. The qualitative differences among these transfer functions are discussed next.

*The Function $I_o(.\,,.)$:* The function $I_o(.\,,.)$ in (25) is substantially different from the function $I_o(.\,,.)$ in (26) and (27). In conventional radiology $I_o(.\,,.)$ is defined over an area called the focal spot and the edges of this intensity distribution are not sharp [14], [17], [20]. On the other hand, in tomography $I_o(.\,,.)$ defines the movement of a point-like X-ray source which is turned on and off over a line which can be straight, circular, elliptical, spiral, hypocycloidal, etc. This means that the blur in conventional radiology is more uniform in all directions than in standard tomography. The uniformity of the blur is the reason why the more complicated X-ray source movements are preferred in tomography; the scanning of an area by an X-ray source has to also be considered in tomography, it has been referred to as areal tomography [40, p. 63]. Of course, the source of X-rays in tomography is also of finite size but the blur that this produces is generally negligible compared to the blur due to its movement.

*Nature of the Process:* The transfer functions in (25), (26), and in the numerator of (27) correspond to radiologic procedures, while the transfer function in the denominator of (27) corresponds to an image processing operation (inverse filtering). This means that the errors and noise are of different nature in each case. In standard tomography additional blur and/or errors occur if the patient moves during the exposure and/or there are mechanical misadjustments. On the other hand, in a tomographic filtration process the effect of a patient moving is not so critical because the exposure time is shorter, but the filtering process is not ideal in practice and noise is amplified by the inverse filter, especially at high frequencies where the gain is greater.

*Transfer Function of the Tomographic Layer:* The transfer functions in (25) and (27) are equal to a constant when $x_i = z_t(= \Delta_2)$, while the transfer function in (26) cannot be identically equal to a constant (except in the limiting case that $z_i = 0$, or $I_o(x, y)$ is an impulse). This is the basic point in the analogy between tomographic filtering and standard tomography.

*Transfer Functions of the Out of Focus Layers:* Even assuming an identical $I_o(.\,,.)$ in every case (which is not practically possible), generally the transfer functions in (25), (26), and (27) for the out of focus layers are not equal. The characterisitcs of the overall transfer functions of the out of focus layers in a tomographic filtration process are considered in Section VI. For an analysis of the transfer functions in standard tomography see, for example, [39].

## V. Quantitative Performance Parameters

The transfer functions contain all the information necessary to compare the various systems. However, they are inconvenient to calculate and compare. The first simplification is to

ignore the phase transfer function and consider only the magnitude transfer function, usually referred to as the modulation transfer function (MTF). Nevertheless, for ease of comparison single number parameters are commonly used in radiology. Tomographic filtering has been compared with standard tomography/zonography and conventional radiology on the basis of the following parameters: the exposure angle, the thickness of the tomographic layer, the rate of change of the MTF, the signal-to-noise ratio, and the patient dose [6], [42]. The conclusion of that comparative assessment is that tomographic filtering can be an improvement over conventional radiology, but cannot achieve the results of standard tomography. The main advantage of tomographic filtering is in reducing the radiation dose to the patient. These analytical results have been corroborated practically by processing both simulated radiographs and actual radiographs [6], [43]. A brief summary of the comparative assessment of tomographic filtering follows.

*Thickness of the Tomographic Layer:* In standard tomography the thickness of the cut is normally defined as the distance between two levels which have a tomographic blurring that is insufficiently large to be noticeable in the presence of the usual radiographic blurrings. This is a subjective definition and it depends on the relative amount of other blurrings such as those due to the focal spot intensity distribution and patient movement. On the other hand, in a tomographic filtration process (TFP) the tomographic blur is based on the focal spot intensity distribution and the blur due to patient movement is negligible because the exposure time is very short.

Hence, the thickness of the cut depends on the extent of the movement of the X-ray source in tomography or the size of the focal spot in a TFP. It is more usual to give the exposure angle rather than the extension of the movement of the X-ray source (or size). The exposure angle is defined as the angle through which the projecting ray of a central point of the plane of cut "moves" during the exposure. In tomography the exposure angle normally ranges from 1-5° (in zonography) to 120-170° (in transversal tomography) [36]. In conventional radiography, and therefore in a TFP, the exposure angle is determined by the size of the focal spot. With a typical focal spot size of 2 mm and focal spot to plane distance of 1000 mm, the exposure angle is about 0.1°. Thus, in terms of the exposure angle a TFP would be closer to zonography than to any other tomographic technique.

When exposure angle is translated to thickness of cut, in standard tomography it is of the order of a few millimeters, in zonography it is on the order of a few centimeters, and a tomographic filtration process even larger. Due to the lack of experimental data conclusive results cannot be given for a TFP [6]. However, it is expected that by using visual workstations for interactive viewing (e.g., with zooming and magnification) the apparent thickness of cut in a TFP could become close to that of zonography. A TFP is an improvement over conventional radiography but it cannot achieve the thin cuts of standard tomography.

*The Rate of Change of the Modulation Transfer Function (MTF):* A measure has been proposed to quantify the contrast between layers after they have been imaged on the film [6]. This is based on the rate of change of the transfer functions in (25), (26), and (27) from layer to layer for a specific type of exposure function $I_o(x_o, y_o)$. Quantitative results were obtained by assuming a Gaussian function. This may not be realistic, but it provides a good basis to compare the performance of the tomographic filtration process with that of standard tomography. When identical exposure functions are considered, the results showed that for layers between the focal spot and the plane at a distance $(d \cdot \Delta_2)/(2 \cdot d - \Delta_2)$ from the film, the transfer function in a TFP varies faster from layer to layer than in the equivalent system using standard tomography. It can be shown that this interval always contains the plane of cut $z_i = \Delta_2$, hence in a region around the tomographic layer a TFP gives better contrast between layers than standard tomography. However, if the normal sizes of the exposure function are taken into consideration (i.e., about 500 mm in standard tomography and about 2 mm in TFP), the performance of standard tomography is by far better because the interval around the plane of cut is negligible.

*The Signal-to-Noise Ratios:* The signal-to-noise ratio (SNR) is defined here as the ratio of the power of the signal from the tomographic layer if it was the only one present in the object and the power of the noise contributed by all other layers. This signal-to-noise ratio provides another measure of the contrast of the image of the plane of cut with respect to the others.

The object being X-rayed, represented by the distribution of linear attenuation coefficients, is considered to be a random process. The power is given by the integral of its power spectral density function. To determine the signal-to-noise ratio the power component due to the image of the tomographic layer ($P_t$) and the noise power due to the other layers ($P_n$) are separated. It is also useful to separate the noise power due to layers between the anode and the tomographic layer ($P_a$) and the noise power due to layers between the tomographic layer and the film ($P_f$). Equation (6) shows how they are related:

$$P = P_t + P_n = P_t + P_a + P_f. \tag{28}$$

Formulas to calculate these powers can be found in [6]. The various signal-to-noise ratios can then be calculated as follows:

$$\mathrm{SNR} = P_t/P_n \tag{29}$$

$$\mathrm{SNR}_a = P_t/P_a \tag{30}$$

$$\mathrm{SNR}_f = P_t/P_f \tag{31}$$

$$\mathrm{SNR} = \frac{\mathrm{SNR}_a \cdot \mathrm{SNR}_f}{\mathrm{SNR}_a + \mathrm{SNR}_f}. \tag{32}$$

Equations (28)-(32) were calculated in about 4000 cases. Table I shows a representative sample of the results—the variation of the signal-to-noise ratio with respect to the nominal thickness of the tomographic layer. To calculate Table I the following parameters were assumed: $d = 1000$ mm, $z_t = 500$ mm, object of thickness 264 mm and positioned at equal distances from film and focal spot, object made of white noise band limited at 5 cycles/mm, and $I_o(x_o, y_o) = \exp(-100 \cdot x_o^2 - 100 \cdot y_o^2)$.

It is clear that the SNR (also $\mathrm{SNR}_a$ and $\mathrm{SNR}_f$) increases with the thickness of the tomographic layer, as expected, because of its definition. Other results have shown that when the object is moved closer to the focal spot or the size of the exposure

TABLE I
THE SIGNAL-TO-NOISE RATIOS VERSUS THE THICKNESS OF THE CUT

| Thickness of the cut (mm) | | 4 | 20 | 40 | 100 | 200 | 240 |
|---|---|---|---|---|---|---|---|
| Standard tomography | SNR | 0.017 | 0.089 | 0.19 | 0.67 | 3.6 | 11.0 |
| | $SNR_a$ | 0.033 | 0.180 | 0.39 | 1.30 | 7.1 | 23.0 |
| | $SNR_f$ | 0.033 | 0.180 | 0.39 | 1.30 | 7.1 | 23.0 |
| Conventional radiography | SNR | 0.015 | 0.081 | 0.18 | 0.60 | 3.1 | 9.8 |
| | $SNR_a$ | 0.036 | 0.190 | 0.43 | 1.50 | 8.3 | 27.0 |
| | $SNR_f$ | 0.026 | 0.140 | 0.30 | 0.99 | 4.9 | 15.0 |
| Tomographic filtering | SNR | 0.013 | 0.068 | 0.15 | 0.48 | 2.3 | 7.4 |
| | $SNR_a$ | 0.045 | 0.240 | 0.55 | 2.10 | 13.0 | 47.0 |
| | $SNR_f$ | 0.018 | 0.093 | 0.20 | 0.62 | 2.8 | 8.7 |

function increases, the SNR increases in standard tomography, but in conventional radiography and tomographic filtering it decreases. When the system parameters are the same (i.e., any column in Table I), $SNR_a$ is maximum for tomographic filtering and minimum for standard tomography. On the other hand, $SNR_f$ and SNR are maximum for standard tomography and minimum for tomographic filtering. This shows that tomographic filters perform better for layers in the object closer to the film. When the tomographic layer is closer to the focal spot, the high pass effect on the layers on the side of the film produce the decrease in SNR through an increase in the noise power.

These measures give only an indication of the performance from a theoretical point of view. In practice, the object is very structured and the effects of noise due to other layers cannot be calculated statistically.

## VI. VARIATION OF THE POINT-SPREAD FUNCTION (PSF) AND THE TRANSFER FUNCTION (TF) WITH DEPTH

To conclude this paper, the effects of tomographic filtering on the images of layers at various depths between the focal spot and the film will be examined in the space domain in terms of the shape of the impulse response or PSF and in the frequency domain in terms of the shape of the overall magnitude response. For simplicity and without loss of generality, one-dimensional functions are considered.

### A. Space Domain

First, a space domain characterization can be provided by the overall impulse response of the TFP. Suppose a focal spot with a Gaussian X-ray intensity distribution, namely,

$$I_o(x) = e^{-\sigma x^2}.$$

The transfer functions and impulse responses of such a system were derived [6]. Fig. 3 shows the overall impulse response of a TFP at various depths $\Delta_1 + t$, for $\sigma = 2$, $d = 1000$ mm, $\Delta_1 = 500$ mm, $-1 < f < 1$ cycles/mm, sampling interval = 1/128 cycles/mm, and several values of $t$ (in mm) as indicated with the plots in Fig. 3. The overall impulse response for the tomographic layer is obviously an impulse and is not shown. It is readily seen in Fig. 3(a)-(d) that between the plane of cut and the focal spot the impulse response is a Gaussian function whose size increases when the distance to the plane of cut increases. On the other hand, between the plane of cut and the film [see Fig. 3(e)-(h)], the impulse response contains side lobes which increase with the distance to the tomographic layer. In general, the wider the impulse responses and the greater the side lobes, the better the contrast between the tomographic layer and the overlaying layers. However, the ripples in the impulse responses for the layers on the film side may introduce artifacts which might mask structures in the other layers.

The reason for the distinctive nature of the impulse responses on each side of the tomographic layer is very simple. On the focal spot side ($t > 0$) the transfer function is a Gaussian function whose inverse transform is another Gaussian function, Fig. 3(a)-(d). On the film side ($t < 0$), however, the transfer function is an inverse Gaussian function which does not have an inverse transform. It was necessary to truncate this ideal transfer function with a frequency domain window (that is, an ideal low-pass filter) with a passband from -1 to 1 cycles/mm.

The analysis presented here could also be applied to investigate the effect of a time or space scaling error in any inverse filtering problem.

### B. Frequency Domain

We now analyze this phenomenon in the frequency domain. Ideally a tomographic filter should have a frequency response such that in combination with the transfer function of the radiologic system, the resulting overall transfer function would be equal to a constant for the tomographic layer and equal to zero everywhere else. In practice, the second condition cannot be met, not even closely. It is the purpose of this analysis to investigate the overall frequency response at different depths.

The overall transfer function for a particular layer is equal to the quotient of the transfer function for that layer without the tomographic filter and the transfer function of the tomographic layer. Evidently, for the tomographic layer the overall transfer function is identically equal to 1. The overall transfer function for other layers is shown in Fig. 4. Since the shape of $H$ is low pass and its bandwidth increases with depth, it is clear that the tomographic filter acts as a low-pass filter for layers between the plane of cut and the focal spot, and as a high-pass filter for layers between the plane of cut and the film.

To fully understand the effects of the process on different layers we must also consider the characteristics of the spectrum of the projected object. Since different layers suffer different magnifications during exposure, the corresponding two-dimensional Fourier transforms of their shadow images are scaled accordingly. Assuming that each layer has approximately the same spectrum, the relative scalings due to magnification are shown in Fig. 5. These different scalings of the shadow images (superimposed on the film) of the layers in the object, suggest a processing technique that will be referred to as *tomographic enhancement* (as opposed to *tomographic restoration*, which has been described in this paper). Indeed, a low-pass filter will enhance the images of layers closer to the focal spot, while a

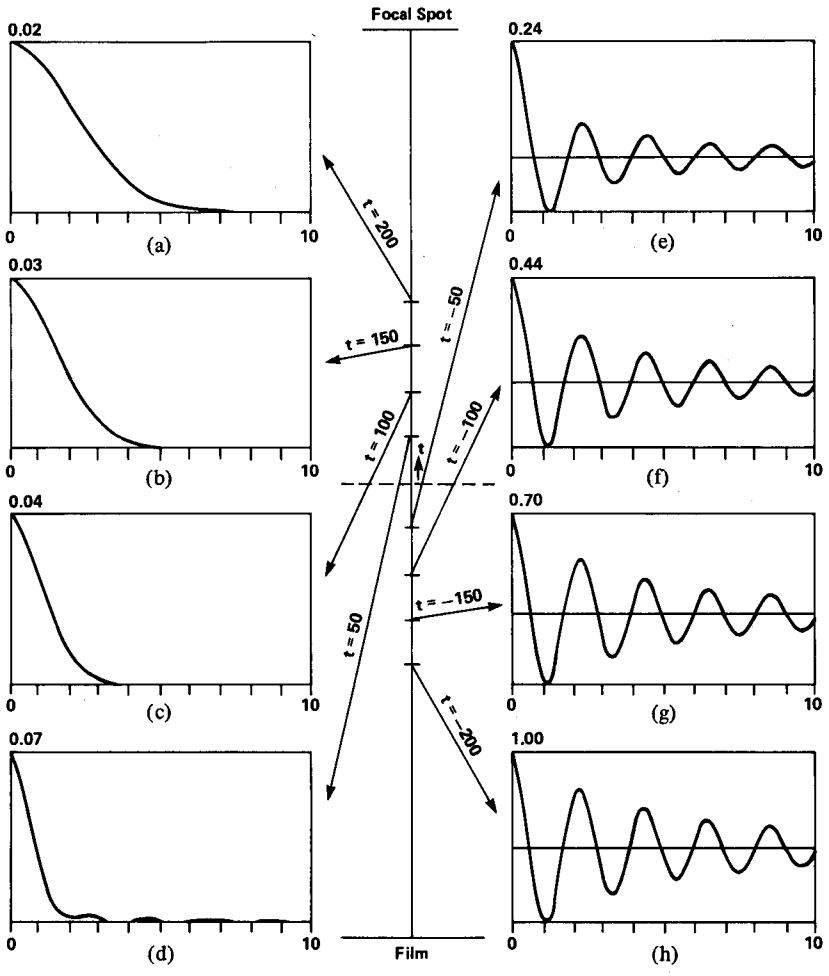


**The focal spot to film distance is 1000 mm.**

**The plane of cut (t = 0) is at 500 mm from the film.**

**The horizontal dimension in the graphs represents distances in mm and the vertical dimension represents normalized amplitudes of the PSF.**

Fig. 3. (a)–(h) Overall impulse responses with a Gaussian focal spot.

Characteristics of the overall transfer function in tomographic filtering

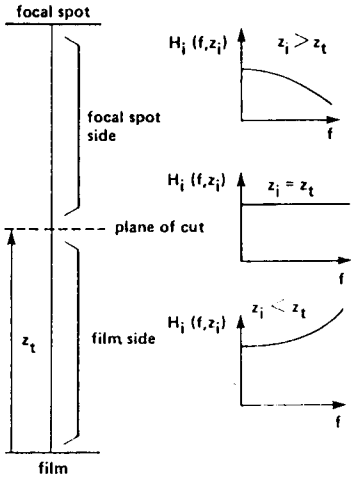


Fig. 4. Variation with depth of the overall magnitude response of a TFP.

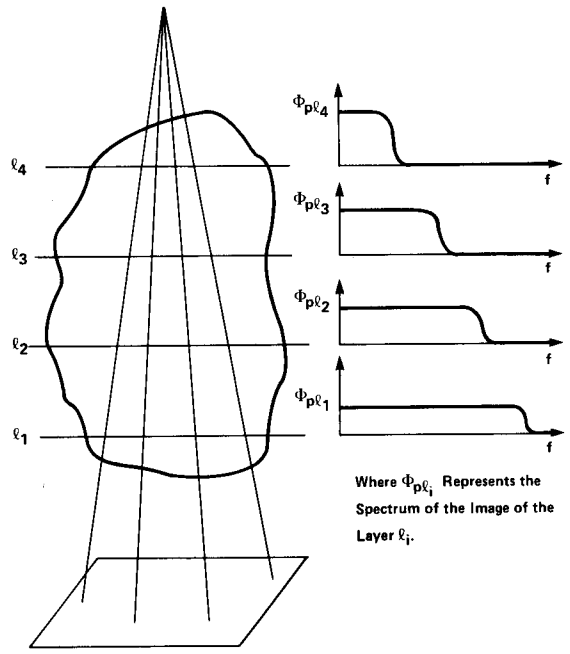


Fig. 5. Scaling of the spectra of the images of layers at various depths.

high-pass filter will enhance the images of layers closer to the film. With bandpass or spectral-shaping filters, selective enhancement of given layers could be realized. While the tomographic filtering technique presented in this paper aims at producing tomograms by filtering radiographs, other techniques described in the past in the literature were aimed at filtering standard tomograms to remove defocus blur (e.g., [40], [44], [45]).

## VII. Conclusions

A TFP is a technique for recovering three-dimensional information from a single radiograph. The mathematics of tomographic filters have been derived and analyzed. The advantages of a TFP are that it can be used with conventional radiography equipment and, by processing a given radiograph with filters with different parameters, additional depth information can be obtained without increasing the patient dose.

The transfer functions of standard tomography, conventional radiology, and a TFP have been derived and compared. It has been shown that a TFP has a low-pass filter effect on the images of layers between the plane of cut and the focal spot and high-pass characteristics on the images of layers between the plane of cut and the film.

## Appendix

### Conversion of a Space-Variant Model into a Space-Invariant One

The radiologic process is space-variant for several reasons [6]. In this Appendix we propose a solution to the problem of lack of parallelism of the focal spot and film planes.

There is a simple way to correct for this type of space variability of the radiologic process in a digital computer. As shown in Fig. 6, the radiologic image can be sampled uniformly and then a new image is calculated by interpolation. This new image is the one that would correspond to a plane parallel to the focal spot; therefore, it has space-invariant properties. The new image can be calculated anywhere in the X-ray field. In order to minimize size distortions we have chosen the plane that, being parallel to the focal spot, passes through the intersection of the center ray and the film plane. With this approach the reconstruction of the object is made on layers parallel to the focal spot. The information required for the conversion is the following: the angle of the focal spot, the focal spot to film distance, and the orientation of the film.

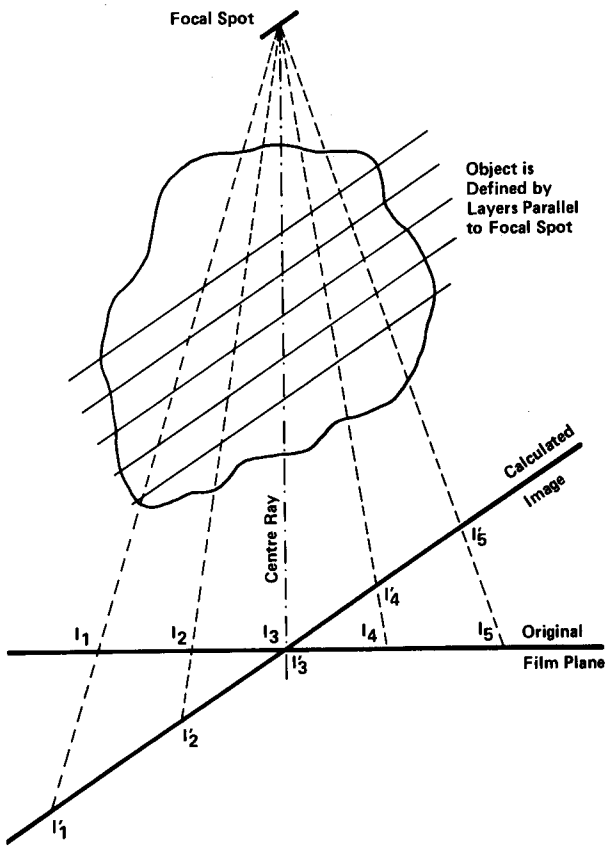


Fig. 6. Conversion of the space-variant model into a space-invariant one.

The relationship between the coordinates $(x, y)$ over the film plane in the space-variant system and the coordinates $(x, y)$ over a plane parallel to the focal spot can easily derived by geometric considerations. Indeed, referring to Fig. 7, since $\overset{\triangle}{FBO} \sim \overset{\triangle}{FAE}$ and $\overset{\triangle}{FOD} \sim \overset{\triangle}{FEC}$, we have

$$\frac{\overline{FO}}{\overline{BO}} = \frac{\overline{FE}}{\overline{AE}}; \quad \frac{d}{x} = \frac{d - \hat{y}\sin\alpha}{\hat{x}}; \quad x = \frac{d\hat{x}}{d - \hat{y}\sin\alpha} \tag{35a}$$

and

$$\frac{\overline{FO}}{\overline{OD}} = \frac{\overline{FE}}{\overline{EC}}; \quad \frac{d}{y} = \frac{d - \hat{y}\sin\alpha}{\hat{y}\cos\alpha}; \quad y = \frac{d\hat{y}\cos\alpha}{d - \hat{y}\sin\alpha}. \tag{35b}$$

Therefore, the intensity distribution $\hat{I}(\hat{x}, \hat{y})$ of an equivalent space-invariant system can be expressed as a function of the intensity distribution $\hat{I}(\hat{x}, \hat{y})$ of the space-variant system as

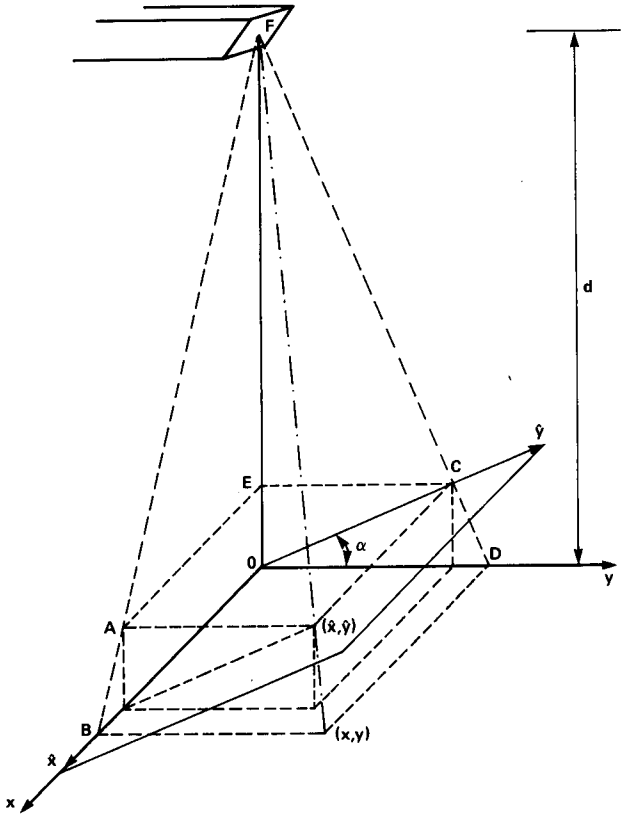


Fig. 7. Relationship between the coordinates on the film plane in the space-variant model and in the equivalent space-invariant model.

follows:

$$\hat{I}(\hat{x}, \hat{y}) = I(x, y) = I\left(\frac{d\,\hat{x}}{d - \hat{y}\sin\alpha}, \frac{d\,\hat{y}\cos\alpha}{d - \hat{y}\sin\alpha}\right). \tag{36}$$

In a practical case (36) would be applied as follows. The radiograph is either sampled at nonuniform intervals as shown in (36) or a new set of samples is obtained by interpolating a uniformly sampled radiograph. This sampling rate should be sufficiently high so that the interpolating error is negligible. The new space-invariant intensity distribution $\hat{I}(\hat{x}, \hat{y})$ is used and processed instead of $I(x, y)$, but taking into account the new geometry of the system, that is the focal spot to plane $\hat{x}, \hat{y}$ distance.

It must be emphasized that this transformation gives a hypothetical image which does not really exist in the actual system but which results in a space-invariant system without loss of information. Indeed, if we wanted to calculate the true intensity in the actual system when the radiation crosses the plane $\hat{x}, \hat{y}$ parallel to the focal spot, derived from the intensity distribution on the plane $x, y$, the inverse square law correction factor should be included to take into account the diverging nature of X-rays. However, if we were to do that we would introduce another source of space variance due to the obliquity of the X-rays on impact over the plane $\hat{x}, \hat{y}$ and therefore the resulting image would be distorted more than it would be corrected.

When the processed film area is small the transformation (36) may not be necessary because the variations of the impulse response within small areas is relatively small. A simple rule has been derived [6] to determine the maximum percent variation $V$ of the extent of the impulse response in the $y$-direction:

$$V = \frac{(y_2 - y_1)\sin\alpha}{d(\cos\alpha) + y_1 \sin\alpha}\ 100 \text{ percent}$$

where $y_1$ and $y_2$ are the ordinates of the film area edges which are perpendicular to the $y$-axis. For example, if $\alpha = 70°$, $d =$ 1000 mm, $y_1 = 50$ mm and $y_2 = 100$ mm, we obtain $V = 12$ percent only. On the other hand, if we consider a larger area, say $y_1 = 50$ mm and $y_2 = 300$ mm, we obtain $V = 60$ percent; hence, in this case some correction would help.

## References


[1] B. G. Ziedses des Plantes, "Body-section radiography: History, image information, various techniques and results," *Australasian Radiology*, vol. XV, no. 1, pp. 57–64, Feb. 1971.

[2] H. J. Trussel, "Processing of X-ray images," *Proc. IEEE*, vol. 69, no. 5, pp. 615–627, May 1981.

[3] R. M. Mersereau, "Digital reconstruction of two-dimensional signals from their projections," Sc.D. dissertation, Dep. Elec. Eng., MIT, Cambridge, MA, Feb. 1973.

[4] J. M. Costa and A. N. Venetsanopolous, "Digital tomographic restoration of radiographs," in *Proc. Conf. Digital Processing of Signals in Communications*, Univ. Technology, Loughborough, Leicestershire, England, Sept. 6–8, 1977, pp. 559–567.

[5] J. M. Costa, "Tomographic filters for digital radiography," *Digital Radiography, Proc. SPIE*, vol. 314, pp. 64–71, 1981.

[6] —, "Design and realization of digital tomographic filters for radiographs," Ph.D. dissertation, Univ. Toronto, Ont., Canada, 1981.

[7] G. A. Krusos, "The amelioration of contrast and resolution of X-ray images using optical signal processing," Eng. Sc.D. dissertation, Columbia Univ., New York, 1971.

[8] K. Rossman, "Image quality," in *Symp. Perception of the Roentgen Image, Radiologic Clinics in North America*, vol. VII, no. 3, pp. 419–433, Dec. 1969.

[9] E. M. Laasonen, "Information transmission in Roentgen diagnostic chains," *Acta Radiologica*, suppl. 280, pp. 1–93, 1968.

[10] R. H. Morgan, "The frequency response function, a valuable means of expressing the informational recording capability of diagnostic X-ray systems," *American J. Roentgenology, Radiation Therapy and Nuclear Medicine*, vol. 88, no. 1, pp. 175–186, July 1962.

[11] K. Doi, A. Kaji, T. Takizawa, and K. Sayanagi, "The application of optical transfer function in radiography," in *Proc. Conf. Photographic and Spectroscopic Optics*, 1964; also in *Japanese Appl. Phys.*, vol. 4, suppl. I, pp. 183–190, 1965.

[12] R. D. Moseley, Jr., and J. H. Rust, Eds., *Diagnostic Radiologic Instrumentation, Modulation Transfer Function.* Springfield, IL: Charles C Thomas, 1965.

[13] B. R. Hunt, "Digital image processing," *Proc. IEEE*, vol. 63, pp. 693–708, Apr. 1975.

[14] K. Doi, "Optical transfer functions of the focal spot of X-ray tubes," *American J. Roentgenology, Radiation Therapy and Nuclear Medicine*, vol. 94, no. 3, pp. 712–718, July 1965.

[15] G. Lubberts and K. Rossmann, "Modulation transfer function associated with geometrical unsharpness in medical radiography," *Phys. Med. Biol.*, vol. 12, no. 1, pp. 65–67, Jan. 1967.

[16] E. Takenaka, K. Kinoshita, and R. Nakajima, "Modulation transfer function of the intensity distribution of the Roentgen focal spot," *Acta Radiologica, Therapy, Physics, Biology*, vol. 7, fasc. 4, pp. 263–272, Aug. 1968.

[17] R. F. Wagner, K. E. Weaver, E. W. Denny, and R. G. Bostrom, "Toward a unified view of radiological imaging systems–Part I: Noiseless images," *Med. Phys.*, vol. 1, no. 1, pp. 11–24, Jan.–Feb. 1974.

[18] E. L. Chaney and W. R. Hendee, "Effects of X-ray tube current and voltage on effective focal-spot size," *Med. Phys.*, vol. 1, no. 3, pp. 141–147, May–June 1974.

[19] G. U. V. Rao and A. Soong, "An intercomparison of the modulation transfer functions of square and circular focal spots," *Med. Phys.*, vol. 1, no. 4, pp. 204–209, July–Aug. 1974.

[20] K. Doi and K. Sayanagi, "Role of optical transfer function for optimum magnification in enlargement radiography," *Japanese J. Appl. Phys.*, vol. 9, no. 7, pp. 834–839, July 1970.

[21] E. N. C. Milne, "The role and performance of minute focal spots

in roentgenology with special reference to magnification," *CRC Critical Rev. Radiol. Sci.*, vol. 2, pp. 269–310, May 1971.

[22] J. B. Minkoff, S. K. Hilal, W. F. Konig, M. Arm, and L. B. Lampert, "Optical filtering to compensate for degradation of radiographic images produced by extended sources," *Appl. Opt.*, vol. 7, no. 4, pp. 663–641, 1968.

[23] G. A. Krusos, "The amelioration of contrast and resolution of X-ray images using optical signal processing," Eng. Sc. D. dissertation, Columbia Univ., New York, 1971.

[24] M. Trefler and E. N. C. Milne, "The diagnostic quality of optically processed radiographs," *Radiology*, vol. 121, no. 1, pp. 211–213, Oct. 1976.

[25] S. Wende, E. Zieler, and N. Nakayama, *Cerebral Magnification Angiography*. New York: Springer-Verlag, 1974, ch. 8.

[26] B. R. Hunt, D. H. Janney, and R. K. Zeigler, "An introduction to restoration and enhancement of radiographic images," Los Alamos Scientific Laboratory, Los Alamos, NM, Tech. Rep. LA-4305, 1970.

[27] B. R. Hunt, "The inverse problem of radiography," *Math. Biosci.*, vol. 8, pp. 161–179, 1970.

[28] D. G. Falconer, "Image enhancement and film-grain noise," *Optica Acta*, vol. 17, no. 9, pp. 693–705, Sept. 1970.

[29] B. R. Hunt and J. R. Breedlove, "Scan and display considerations in processing images by digital computer," *IEEE Trans. Comput.*, vol. C-24, no. 8, pp. 848–853, Aug. 1975.

[30] L. Biberman, Ed., *Perception of Displayed Information*. New York: Plenum, 1973.

[31] A. Rose, "A unified approach to the performance of photographic film, television pickup tubes, and the human eye," *J. Soc. Motion Picture Eng.*, vol. 47, no. 4, pp. 273–294, Oct. 1946.

[32] H. C. Andrews, "Monocrome digital image enhancement," *Appl. Opt.*, vol. 15, no. 2, pp. 495–503, Feb. 1976.

[33] B. S. Lipkin and A. Rosenfeld, Eds., *Picture Processing and Psychopictorics*. New York: Academic, 1970.

[34] E. L. Hall, R. P. Kruger, S. J. Dwyer, III, D. L. Hall, R. W. McLaren, and G. S. Lodwick, "A survey of preprocessing and feature extraction techniques for radiographic images," *IEEE Trans. Comput.*, vol. C-20, no. 9, pp. 1032–1044, Sept. 1971.

[35] W. J. Meredith and J. B. Massey, *Fundamental Physics of Radiology*, 2nd Ed. Bristol, Great Britain: John Wright & Sons Ltd., 1972.

[36] A. Berrett, S. Brünner, and G. E. Valvassory, Eds., *Modern Thin-Section Tomography*. Springfield, IL: Charles C Thomas, 1973.

[37] D. Westra, "Zonography. The narrow-angle tomography," thesis, Excerpta Medica Foundation, Amsterdam, The Netherlands, 1966.

[38] K. Lindblom, "On microtomography," *Acta Radiologica (Stockholm)*, vol. 42, p. 465, 1954.

[39] S. C. Orphanoudakis and J. W. Strohbehn, "Mathematical model of conventional tomography," *Med. Phys.*, vol. 3, no. 4, pp. 224–232, July–Aug. 1976.

[40] P. Edholm, "The tomogram, its formation and content," *Acta Radiologica (Stockholm)*, suppl. 193, 1960.

[41] S. C. Orphanoudakis, J. W. Strohbehn, and C. E. Metz, "Linearizing mechanisms in conventional tomographic imaging," *Med. Phys.*, vol. 5, no. 1, pp. 1–7, Jan.–Feb. 1978.

[42] J. M. Costa, A. N. Venetsanopoulos, and M. Trefler, "Evaluation of digital tomographic filters," Dep. Elec. Eng., Univ. Toronto, Ont., Canada, Communications Tech. Rep., 1983.

[43] —, "Design and implementation of digital tomographic filters," this issue, pp. 89–100.

[44] J. W. Strohbehn, C. H. Yates, B. H. Curran, and E. S. Sternick, "Image enhancement of conventional transverse-axial tomograms," *IEEE Trans. Biomed. Eng.*, vol. BME-26, no. 5, pp. 253–262, May 1979.

[45] M. W. Vannier and R. G. Jost, "Digital processing of conventional tomograms," *Appl. Opt. Instrum. Medicine IX, Proc. SPIE*, vol. 273, pp. 350–356, 1981.